RSC Advances

ROYAL SOCIETY OF CHEMISTRY

www.rsc.org/advances

Bioactive and porous-structured nanocomposite microspheres effective for cell delivery: A feasibility study for bone tissue engineering

Jeong-Hui Park [a,b], Mi-Kyung Kim [a,b], Ahmed El-fiqi [a,b], Seog-Jin Seo [a,b], Eun-Jung Lee [a,b], Joong-Hyun Kim [a,b], Hae-Won Kim [a,b,c,*]

[a]Department of Nanobiomedical Science & BK21 PLUS NBM Global Research Center for Regenerative Medicine, Dankook University, Cheonan, 330–714, Republic of Korea

[b]Institute of Tissue Regeneration Engineering (ITREN), Dankook University, Cheonan, 330–714, Republic of Korea

[c]Department of Biomaterials Science, School of Dentistry, Dankook University, Cheonan, 330–714, Republic of Korea

---

* Corresponding author: Prof. H.-W. Kim

E-mail) kimhw@dku.edu; Tel) +82 41 550 3081; Fax) +82 41 550 3085

For: **RSC Advances**

Abstract:

A novel nanocomposite microspherical cell-carrier system was developed to populate stem cells and to stimulate their osteogenesis for bone tissue engineering. Biopolymer-based composition incorporating bioactive glass nanoparticles (BGn) was spherodized with size of hundreds of micrometers. In particular, the morphology of the microcarriers was porous-structured with the help of camphene. The nanocomposite porous microcarriers showed excellent surface bioactivity, easily forming apatite mineral in vitro. Rat mesenchymal stem cells populated well onto the porous microcarriers, exhibiting tight anchorage with underlying surface and active spreading and proliferation behaviors. The surface-mineralization significantly improved the cell proliferative potential. *In vivo* tests in rat calvarial defects confirmed excellent tissue compatibility of the microcarriers. The BGn incorporation and the surface mineralization significantly improved the ingrowth of cells and tissues within the pore channels and the consequent bone regeneration. In particular, the mineralized surface showed enhanced capacity to deliver protein molecules, loading at higher quantity and releasing them more slowly than the unmineralized surface. Results demonstrated the feasibility of the nanocomposite porous microspheres as a potential cell delivery system for bone tissue engineering.

Keywords: Nanocomposites; Porous microsphere; Cell carriers; Bioactive surface; Bone regeneration

1. Introduction

Spherical microparticulates ('microspheres') are an attractive form of biomaterial scaffolds that find usefulness in drug delivery and tissue engineering. Microspheres have been used as an effective three-dimensional (3D) substrate for the population and expansion of mammalian cells [1,2]. Compared to the pre-shaped 3D foam scaffolds, this spherical form sized with tens to hundreds of micrometers can be easily adapted into defective sites, often allowing injectable implantable system for minimally invasive maxillofacial and orthopedic surgery [3]. Along with the chemical properties, including surface reactivity and degradability, the microsphere geometry, such as surface roughness and pore structure is considered to be important in determining the efficacy to load cells and further to allow their proper differentiation into target tissues [4,5].

Among else, a porous structure has potential merit, considering the loading of cells as many as possible by providing them anchorage surface sites and a space for multiplication [4-6]. When compared to the nonporous microspheres where cells can only be present on the outer surface, porous microspheres can enable cells to migrate within the pore structure [1,4]. Furthermore, the cells within the pores can experience different microenvironmental conditions from those present on the outer surface with regard to fluid circulation, nutrient variations and cell-to-cell contacts [1]. In this manner, the pore structure is considered to be important in improving the ability of the microspheres to hold and deliver cells and to induce their functional differentiation.

Some interesting studies have developed porous microspheres of biopolymers utilizing a range of methodologies [6-9]. Our group has also developed porous biopolymer microspheres by introducing a camphene, a hydrocarbon volatile chemical with extremely high freezing point (around 40 ^{o}C) [4,9]. Although the biopolymers are not toxic to cells to be loaded, the poor surface properties (i.e, low hydrophilicity, water permeability and protein adhesion ability) largely hamper initial cellular reactions and the subsequent cell loading and proliferation [4,10,11].

It is possible to increase the bioactivity of the biopolymers by either incorporating bioactive materials (such as bioactive nanoparticles) inside or tailoring the surface with adhesive proteins or bone mineral phase. Here we focus on incorporating bioactive glass nanoparticles (BGn) within the biopolymer microcarriers for bone regeneration purpose. BGn have recently been considered an attractive source of bone regenerative material that has nanoscale morphology (generally < 100 nm) while retaining excellent bone bioactivity, such as ion-eluting property and apatite bone mineral

apposition [12-14]. While the BGn-incorporated biopolymer microcarriers are supposed to be a useful 3D culture matrix for bone-associated cells, they also thought to effectively induce apatite bone mineral phase on the microcarrier surface, which is believed to provide valuable surface conditions for cells and proteins and even therapeutic molecules that can be tethered [15-17]. When the microcarriers deliver therapeutic functions by tethering proteins on the surface, the effectiveness of the scaffolds in bone regeneration should be significantly improved.

Therefore, the aim of this study is to develop novel microcarriers with bioactive composition and porous morphology for bone regeneration. BGn were incorporated within the polycaprolactone/poly(lactic acid) (PCL/PLA) blend biopolymer to improve bone-bioactivity, and the surface was mineralized with apatite phase. The efficacy of the porous microcarriers in loading tissue cells and their expansion for tissue engineering *in vitro* was assessed, and the bone forming ability *in vivo* was investigated. Furthermore, the performance of the surface-mineralized microcarriers in loading and delivering protein molecules was also briefly addressed. It is hoped that this new type of bioactive porous microcarriers find great usefulness in directly filling bone defects or in delivering cells for tissue engineering in conjunction with therapeutic potential.

The scheme of this study is schematically shown in **Fig. 1**. As depicted, the nanocomposite solution is made of PCL/PLA blend and BGn at varying concentrations in chloroform, which is combined with camphene to introduce highly porous structure. The solution is emulsified in surfactant-water bath while gentle stirring to produce spherical-shaped microparticles. During the emulsification, camphene solidifies accompanied by a solvent evaporation to form a bi-continuous network with the polymer phase. Further stirring allows the sublimation of camphene to leave an interconnected pore channel and the surrounding polymer-networked microcarrier. The addition of BGn allows ease of apatite mineral induction on the surface of the porous microcarrier, producing surface-mineralized microcarrier. The mineralized surface is subsequently incorporated with proteins to improve the surface more mimicking the bone extracellular matrix (ECM) or to provide therapeutic efficacy to regulate stem cells for *ex vivo* tissue engineering or to heal/regenerate bone tissues when directly implanted.

2. Materials and methods

2.1. Preparation of microcarriers and mineralization

As the bioactive nanoparticle component, BGn were produced. The preparation of the BGn was well described in our previous work [14]. In brief, mesoporous binary composition ($85SiO_2/15CaO$ in mol %) was synthesized by ultra-sound assisted base-catalyzed sol-gel method where polyethylene glycol (PEG) was used as a template. Within a solution of PEG (pH adjusted to 12.5 with NH_4OH) and $Ca(NO_3)_2.4H_2O$, tetraethyl orthosilicate (TEOS) dissolved in methanol was added drop-wise by applying a high-power ultra-sound using a Sonoreactor (LH700S, Ulsso Hitech). The output power was 220 W in a 10-s on/10-s off cycle for 20 min. After 24 h, the white precipitate was separated by centrifugation at 5,000 rpm, washed, re-dispersed with de-ionized water and ethanol, and then dried at 70° C. Samples were then calcined at 700° C in air for 5 h. The nanostructure of the BGn was observed by scanning electron microscopy (SEM; TESCAN, MIRA II LMH) and transmission electron microscope (TEM; JEM-3010, JEOL).

As the polymeric phase for the microcarriers, PCL (Mw = 80,000, Aldrich) and PLA (L,DL-form, Boeringer Ingelheim) blends were used. In a preliminary study, varying ratios of the two polymers were blended in chloroform, dried into films and the contact angle (hydrophilicity) and cell adhesion property were observed. Moreover, the composition allowing the generation of a porous structure within the microcarrier was chosen. Based on this, a composition of PCL/PLA blended at 3:1 was selected to be an optimal. The polymer blend was dissolved in chloroform at 10 % w/w. Within the solution, BGn produced were added at various concentrations (2, 5 and 10% with respect to polymer blend by wt.) with vigorous stirring. As a porogen, camphene ($C_{10}H_{16}$, Sigma-Aldrich) was added at camphene/material = 8, a ratio proper to produce well-developed porous structured microspheres. The prepared material-camphene solution was added dropwise into a water bath containing 2 wt% poly(vinyl alcohol) (PVA, Sigma-Aldrich) while stirring at a constant speed. During stirring, solidification of material occurred and after this, the solution was stirred for additional 24 h to harden the microcarriers due to the solvent evaporation and to introduce pore channels assisted by the sublimation of camphene. The nanocomposite microcarriers were washed thoroughly with ice-cooled distilled water through a Millipore filter. The obtained microcarriers were further freeze-dried for further treatments and characterizations.

The porous microcarriers were subsequently immersed in an accelerated simulated body fluid (2xSBF) at 37 °C for periods of up to 7 days while gentle stirring [18]. At each selected time point, the microspheres were gathered and examined by SEM and Fourier-transform infrared (FTIR)

spectroscopy to detect the apatite mineralization. In particular, the mineralized microcarriers for 7 days were used for further biological experiments.

2.2. Cell culture and proliferation

The ability of the developed microcarriers to support tissue cells, aiding initial anchorage and subsequent proliferation during *in vitro* culturing, was examined using bone marrow mesenchymal stem cells (MSCs) derived from rats. The protocols of MSCs isolation and maintenance were detailed in our previous works [19,20]. All protocols involving animals were approved by the Animal Care and Use Committee of Dankook University. The harvested product was then centrifuged, and the supernatant was collected and suspended within a culture flask containing a normal culture medium; α-minimal essential medium (α-MEM) supplemented with 10% fetal bovine serum (FBS) and 100 U/ml penicillin and 100 mg/ml streptomycin, in a humidified atmosphere of 5% CO_2 in air at 37°C. After incubation for 1 day, the medium was refreshed and cultured until the cells reached near confluence. After subculture and maintaining in the normal culture condition, cells at 2–3 passages were used for further tests.

Approximately 40 mg of microcarriers were placed onto a Transwell membrane which was contained in each well of 24-well plates to form a monolayer covering the membrane surface and 20,000 cells per well were seeded on top of the microcarriers. After predetermined period, (3 h, 3 and 7 days), cell number was quantified by cell counting kit (CCK-8, Dojindo Molecular Technologies). The medium was replaced with 200 μl of serum-free medium, and followed by the addition of 20 μl of CCK-8 solution (Dojundo, Japan). The reagent was left to react for 2 h and then the reactant was read at 450 nm using UV-vis spectrophotometer.

Cell morphology was observed by confocal laser scanning microscopy (CLSM; LSM 510, Zeiss). For this, at each culture period, the cells were fixed with 4% paraformaldehyde solution and stained with Alexa Fluor 546 conjugated Phalloidin (Molecular Probes) and Prolong Gold antifade reagent with DAPI (Molecular Probes), and then the fluorescence signals were visualized.

2.3. In vivo study in rat calvarium defect

In vivo tissue reactions of the microcarriers were assessed under the rat calvarium defect [5]. Ten-week-old male Sprague-Dawley rats were used. Animal surgery protocol was performed in

accordance with the Animal Care and Use Committee in Dankook University, South Korea. Animals were anaesthetized by means of intramuscular injection using ketamine (80 mg/kg) and xylazine (10 mg/kg). An incision was made in the anterior region of the calvarium and a 5 mm diameter critical-sized full-thickness bone defect was prepared using a trephine drill under continuous sterile saline irrigation. Different types of microcarriers (biopolymer, 10%BGn-added, and its mineralized microcarrier) were implanted within the calvarium defect. Soft tissues were closed and sutured to achieve primary closure. Four and eight weeks after implantation, the animals were sacrificed. The area of the original surgical defect and surrounding tissues were removed *en bloc*, and fixed in 10 % neutral formalin solution and then decalcified.

For histologic assays, tissues were embedded in a paraffin block, and then serial-sectioned using a microtome (LEICA^{TM}) with approximately 5 μm thickness and mounted on microscope slides. Slides with tissue sections were deparaffinized and hydrated through xylene and alcohol series. The tissue slides were stained with hematoxylin & eosin (H&E) and viewed under an optical microscope for the histological observation.

The formation of new bone within the defect region was quantified by monitoring with Micro-CT (Skyscan 1072; Skyscan, Aartselaar, Belgium). The harvested specimens were scanned with each frame exposure for 20 ms. Scanning was performed in the direction parallel to the coronal aspect of the calvarial bone surrounding the defect area. A cylindrical region of interest (ROI) was precisely positioned over the center of the single defect, enclosed all the new bone within the defect site. Micro-CT images were reconstructed over a ROI using CTAn (Skyscan) and the data was analyzed. The total volume of newly formed bone within the ROI was measured using 3D images by assigning a threshold for total bone content (including trabecular and cortical ranges) and subtracting any contributions from the scaffolds, which were determined from the samples as-implanted. Replicated samples for each group were measured and total volume of neo-bone formation was representatively reported.

2.4. Cytochrome C loading and release

The capacity of the microcarriers to incorporate biological molecules and further to release them was assessed using a model protein cytochrome C (cyt C) because it has molecular size and charge properties similar to those of biological growth factors such as basic fibroblast growth factor

[21,22]. Cyt C (Sigma-Aldrich) dissolved in PBS (500 μg/ml) was adsorbed onto the 3 mg of microcarriers with different compositions (polymer microcarrier or 10BGn-added microcarriers either mineralized or not) within PBS for 6 h by gentle agitation. After the adsorption, the microcarriers were sediment down, and the cyt C adsorbed onto the microcarriers was quantified by measuring the cyt C amount remained in the supernatant in terms of UV-vis spectrophotometeric analysis at 408 nm. For the release test, 100 mg of the cyt C-loaded microcarriers were introduced in each well of 24-well plates containing 1 ml PBS. After incubation at 37 ^{o}C the supernatant solution was gathered every predetermined time point, and then assayed. At each time point, PBS was refreshed for the next run. The release profile of cyt C from the microcarriers was monitored over a week.

2.5. Statistics

Data are presented as mean and one standard deviation. Statistical analysis was carried out using one-way analysis of variance and significant level was considered at $p < 0.05$.

3. Results

3.1. Characteristics of nanocomposite porous microcarriers

The SEM image of the porous structured biopolymer microcarrier with PCL/PLDLA blended at 1/3 ratio is shown in **Fig. 2**. Spherical particles with sizes of hundreds of micrometers were well produced and a highly macroporous structure with pores sized approximately 50-100 μm was created. The pore generation was facilitated by the use of camphene which solidifies to form bi-continuous network with the polymer blend and then rapidly sublimates during the spherodization process. The blend of PCL/PLDLA at a ratio of 1/3 was found optimal in terms of spherodization and hydrophilicity; increasing PLDLA content reduced the pore structuring whilst enhanced hydrophilic nature, giving an optimal blending ratio of 1/3.

Based on the porous structuring of the PCL/PLDLA microcarriers, we incorporated BGn within the biopolymer blend at varying concentrations (2, 5 and 10%). The image of BGn (with a composition 15Ca/85Si) produced by an ultrasound-assisted sol-gel process was taken by SEM and TEM (**Fig. 3a,b**). Nanoparticles with spherical form were well generated with sizes of ~80-100 nm. TEM image showed mesoporous characteristic of the nanoparticles. The excellent apatite forming

ability of the BGn was also confirmed by immersion of the BGn in SBF. SEM and TEM images showed the profound mineralization behavior of apatite nanocrystallites (**Fig. 3c,d**).

The BGn was then incorporated within the PCL/PLDLA solution, which was subsequently formulated into a porous microsphere using the conditions same as those for PCL/PLDLA. The nanocomposite solutions showed stable emulsion status without phase separation or sediment down of the nanoparticles **(Fig. 4a)**, thus the BGn is considered to homogeneously disperse within the polymer matrix after the microsphere formation. SEM images of the BGn-added nanocomposite microcarriers showed the formation of spherical particles with sizes of hundreds of micrometers and the pore generation through the microspheres with sizes over 50-100 μm. The microsphere and pore images were similarly observed for both 2%BGn (**Fig. 4b**) and 10%BGn (**Fig. 4c**). When a much higher content of BGn was added (20%BGn), the pore structuring was greatly hampered (not shown here). The FT-IR spectra of the microspheres showed the intensity of chemical bands (Si-O-Si) related with BGn increased with increasing BGn content (**Fig. 4d**, indicated as arrows).

The i*n vitro* apatite forming ability of the nanocomposite porous microcarriers was examined by immersion in 2xSBF. Microcarriers without BGn couldn't induce mineral phase during the immersion even for up to 14 days (**Fig. 5a**). However, with the BGn addition, mineralized crystals were substantially developed on the outer and inner surface of the microcarriers (**Fig. 5b**). The mineralization degree increased with increasing BGn concentration as well as immersion time. The onset of mineralization detectable by SEM was approximately 7 days, 5 days and 1 day in 2%, 5% and 10%BGn, respectively. The mineralized phase was examined by FT-IR spectrum which showed the development of phosphate bands (dotted line) related with apatite (**Fig. 5c**). XRD pattern of 10%BGn before and after 7 days of immersion also showed the development of poorly crystallized apatite phase after the immersion (**Fig. 5d**). While this mineralization process is considered to provide information on the improved ability of the BGn-added microcarriers to inducing apatite mineral, it is also possible to utilize the mineralized microcarriers for bone tissue engineering as the mineralized surface provides effective substrate conditions for cells to grow and differentiate. Therefore, subsequent biological assays were performed using both the mineralized and unmineralized 10%BGn microcarriers.

3.2. In vitro and in vivo biological responses

As the developed microcarriers are of use as cell carriers for tissue engineering, we first assessed the ability to support cellular adhesion and growth of the microcarriers. Rat MSCs were cultured on the 10%BGn microcarriers either with or without the surface-mineralization and the cell proliferation rate was measured. Cells initially adhered at comparable level onto both types of microcarriers. However, the cell proliferation rate on the mineralized microcarriers became significantly higher than that on the nonmineralized microcarriers during culture for 3 and 7 days (**Fig. 6a**), which is considered to be reasoned that the apatite mineral phase underlying the cells would favor the cell growth. The CLSM image showed the MSCs adhered initially, and then grew and proliferated actively on the microcarriers with increasing culture time, and reflected the different cell growth kinetics of the two types of microcarriers (**Fig. 6b,c**).

The *in vivo* tissue compatibility and bone forming ability of the porous microcarriers were investigated after implantation of the microcarriers in rat calvarium defect for 4 and 8 weeks. H&E stained histological findings revealed the formation of tissues well within the defect region, surrounding the microcarriers. For biopolymer group at 4 weeks, although the tissue formation was well noticed around the microcarriers, there was very limited bone tissue ingrowth within the pore channels of the microcarriers. On the other hand, for 10%BG and its mineralized groups at 4 weeks, the new bone formation was well evidenced even within the pore channels (**Fig. 7**). Bone ingrowth behaviors were more pronounced at 8 weeks, filling most of the pore parts while leaving very small areas of the microcarriers, particularly for 10%BGn and its mineralized groups. There was no noticeable histological difference between 10%BGn and the mineralized groups. The bone formation was also monitored by micro-CT and the neo-bone volume % was quantified (**Fig. 8**). Results presented significant improvement in the 10%BGn and mineralized groups compared to biopolymer group, at both 4 and 8 weeks. The mineralized group appeared to show slightly higher level than 10%BGn at 4 weeks. This *in vivo* study confirmed the effective role of the BGn and the mineralized phase on the surface in improving the tissue and bone ingrowth within the generated pore channels of the microcarriers.

3.3. Protein loading and delivery capacity

Next we focused on the additional roles of the mineralized phase on the microcarrier surface in incorporating biological protein molecules, which is considered to be effective in finding usefulness

of the microcarriers for protein delivery. Cytochrome C (cyt C), chosen as the model protein, was adsorbed onto the different microcarrier groups (polymer, 10%BGn, and its mineralized group). Cyt C adsorption was significantly higher on the mineralized microcarrier than on the unmineralized microcarrier or biopolymer microcarrier (almost twice in quantity, as shown in **Fig. 9a**).

Subsequent release test of the cyt C from the microcarriers was performed in PBS for periods of up to 7 days (**Fig. 9b**). The cyt C release from the biopolymer microcarrier was rapid initially (~40% release within 12 h), and substantially slowed-down thereafter (~10% release) with almost complete release as early as at 3 days. Approximately 50% of cyt C initially loaded was however washed out during the preparation of samples for the release study, as the total release amount was only ~50% of the initial loading, implicating half of the protein molecules was loosely bound to the biopolymer surface. The cyt C release from the unmineralized microcarrier (10%BGn) was a bit more sustainable; ~60% of cyt C being released during 12 h, additional ~30% cyt C being released further up to 3 days with almost complete release having a plateau. Compared to biopolymer microcarrier, most of the loaded cyt C was shown to release from the 10%BGn without a loss. The cyt C release from the mineralized microcarrier showed a highly sustained pattern, extending the continual release for up to 7 days; ~45% of cyt C being released during 12 h, additional 40% of cyt C being released further up to 3 days, and additional 15% of cyt C being released up to 7 days, and thus finally almost all of the loaded cyt C being released. In particular, the release profile from the mineralized microcarrier appeared to be diffusion-controlled. These results suggest the ability of the mineralized microcarriers to sustainably release the cyt C molecules over 7 days.

4. Discussion

Microspherical particulates have shown great promise as the 3D scaffolding materials for the cultivation and expansion of tissue cells. Compared to the pre-fabricated block scaffolds, the microspheres can adopt easily to defect sites and allow on-site delivery in the form of injectable device. Particular merit in regenerative medicine is the culture of stem cells *ex vivo* to expand and differentiate them to achieve tissue-equivalent constructs and further to find *in vivo* implantation. For this use as stem cell carriers, the morphological feature, particularly porous structure is considered of highly importance as the pore space can host stem cells at large population. Furthermore, the surface properties need carefully considered to provide cells proper substrate conditions to anchor to, spread

on and then differentiate into an osteogenic lineage which is beneficial for achieving bone analogs and *in vivo* bone formation.

Considering these aspects of the microcarriers, here we implemented bioactive microcarriers with porous structure. The pore structuring was possible by introducing camphene, which initially forms a bi-continuous phase with matrix materials via solidification and then sublimes easily, creating networked pore channels. The process is undertaken simply in one pot through an oil-in-water emulsion method, signifying another merit of this porous structuring of microcarriers. As the basic composition of the microcarriers, PCL/PLDLA blend solution was chosen. Compared to pure PCL, the blend with PLA, like PLDLA improves water affinity (hydrophilicity) and the possible hydrolytic degradability [23,24]. Our previous work on PCL porous microspheres using camphene raised a drawback of hydrophobic property of PCL surface, limiting the utility in water-soaking and cell seeding [25]. Therefore, the addition of PLDLA at least, improves the cell affinity, and possibly the hydrolytic degradability of the microcarriers. However, the introduction of PLDLA was observed to be limited up to 1/3 (PCL/PLDLA) as the blending above this resulted in disintegration in pore generation within the microcarriers.

With particular aim at hard tissue engineering, a novel bone-bioactive inorganic component, nBG was incorporated into the blend biopolymer microcarrier. The nBG used in this study has previously shown excellent *in vitro* bioactivity, exhibiting rapid and profound induction of bone mineral-like apatite phase (also shown in TEM and SEM images after SBF immersion in this study) [14]. The addition of nBG at relatively small concentrations (up to 10% by wt.) preserved well the porous structure of the biopolymer microcarriers, which however, was affected greatly at higher BGn concentration (20%), and this might be due to the increase in hydrophilicity of the matrix phase and thus the increase in interfacial instability in forming bi-continuous network with camphene.

The role of BGn added to the microcarriers was initially evidenced in the apatite mineralization in SBF. The mineralization process was accelerated almost linearly with the BGn incorporation (Fig. 5). The release of calcium ions from BGn should increase the supersaturation of the Ca-and P-containing ionic medium which in turn accelerates the precipitation of calcium-phosphate minerals. In the course of the mineralization, the BGn present on the outermost surface of the microcarriers should first take actions to release calcium ions, however, the BGn at the subsurface embedded within the polymer phase will also involve in this process later when the polymer degrades.

Therefore, the PLDLA component used in the blend with PCL possibly enhance this mineralization behavior of the microcarriers. For the case of 10%BGn, the mineralization was so fast that the complete coverage of microcarrier surface was achieved as early as 5-7 days. Herein, we made use of this rapid and easy mineralization process in modifying the microcarrier surface with mineral phase. Although the BGn-added microcarriers can find great usefulness, the mineral-surfaced microcarriers are also considered of merit in providing matrix conditions effective for stem cells to adhere and grow and further to differentiate into an osteogenic lineage. An *in vitro* experiment of MSCs culturing on the mineralized microcarriers showed the mineralized surface favorably provided substrate conditions for the cells to adhere tightly and spread actively possibly helping cell mitosis (Fig. 6). In fact, significant improvement in cell proliferation was noticed by the mineralization. The nanocrystalline mineral phase might provide nano-roughened surface conditions, stimulating cellular proliferation. While more studies are considered needed to confirm the mechanistic role of mineral surface in cell mitosis and proliferation, some previous works have also reported similar effects on osteoblasts and stem cells [26,27].

We next sought to determine if the nanocomposite porous microcarriers were effective in bone regeneration. *In vivo* experiments in rat calvarium critical-sized defect demonstrated well the promising role of the microcarriers in scaffolding for osteoconduction (Figs. 7 and 8). Polymeric microcarriers also showed tissue compatibility and scaffolding effects, directing tissue ingrowth around the spheres with minimal inflammatory reactions. However, many of the porous inner space of the microcarriers were not readily filled with bony tissue, suggesting a limited role of the composition in the complete and homogeneous osteoconduction. However, the addition of 10%BGn to the polymeric composition substantially improved the ingrowth of cells and tissues into the inner pore channels and the subsequent bone tissue formation. It is believed that the added-BGn should improve the surface property such as hydrophilicity which might help cellular ingrowth; moreover, the possible release of ions from BGn such as calcium and silicon should positively affect the initial cell ingrowth and subsequent tissue formation such as blood vessel formation and bone mineralization. In fact, the positive roles of calcium and silicon ions in stimulating proliferation of bone cells and their maturation and calcification *in vitro* have been well documented [28-30]. Although the exact amount of the released ions from the microcarriers was not measured, a proper range of doses that stimulates cellular growth is envisaged.

Together with this BGn-added microcarrier, the surface-mineralized microcarrier also demonstrated substantial improvement in the cellular ingrowth and bone formation within the pore channels. The neo-bone formation quantified revealed significantly higher levels in both of the10%BGn-added and its mineralized microcarrier than in pure biopolymer microcarrier, confirming the cellular ingrowth occurred earlier in the BGn-added and mineralized microcarriers had positively affected the bone regeneration. As to the surface-mineralization effect, a more rapid tissue ingrowth appeared to occur on the mineralized microcarriers, particularly at earlier time point (4 weeks) which became similar at 8 weeks, suggesting some effective roles of the mineral phase in the early bone formation. It is thought that the mineral phase would stimulate initial tissue reactions such as osteoblasts and/or endothelial cells engrafting and their proliferation during *in vivo* healing process, and this earlier effect was also noticed *in vitro* in the improved MSCs proliferative potential on the mineralized microcarriers. For the mineralized microcarrier, the ionic release and the consequent effects are also expected as it also contains 10%BGn; however, due to the presence of thin outer mineral layer, the ionic release will be lower when compared to the case in non-mineralized microcarrier. Thus the bone formation results should be interpreted considering the combined effects of both ionic release and initial mineralized matrix conditions. As clarified in the *in vivo* bone forming ability, the addition of BGn significantly improves the cell and tissue ingrowth within the porous channels and the subsequent maturation into hard tissues. The post-mineralization of the BGn-added microcarriers also provided effective scaffolding conditions, allowing cellular migration, proliferation and bone formation.

Although the mineralization effect was not so significantly revealed in the *in vivo* bone formation, an impact was evidenced in the ability to incorporate biological proteins. Cyt C, first tested as a model protein, was well adsorbed onto the mineralized microcarriers with significantly higher incorporation amount than the non-mineralized microcarriers (Fig. 9). The negative-charged apatite crystallites (with surface ζ-potential around -10 mV) with highly nano-roughened topology should provide active adsorption sites for the highly positive-charged cyt C, allowing possible ionic interactions and thus facilitating slow release of the molecules, which was subsequently noticed in the release pattern, with a profile of slow release up to a week without exerting initial burst release effect. Based on this cyt C study, we can surmise the possible loading and delivery behaviors of the proteins, particularly growth factors since many growth factors have similarities with cyt C in terms of molecule

size and charge property. The protein loading and release results support the possible efficacy of the mineralization of the bioactive microcarriers when utilizing the microcarrier systems for delivering therapeutic molecules. On the one hand, if stem cells are cultivated on the microcarriers which are pre-loaded with relevant biomolecules such as growth factors, a direct regulation of stem cells cultured on the microcarrier in timely and sustainable manner is envisaged; on the other hand, when the microcarriers loaded with therapeutic molecules are directly implanted into bone defects, the therapeutic efficacy will stimulate bone regeneration (as schemed in Fig. 1). Therefore, the applications of growth factors that are relevant to bone regeneration in this mineralized microcarrier system will be a promising approach for future study when we aim to make full use of the porous microcarriers with improved therapeutic potential for bone tissue engineering.

5. Conclusions

Bioactive and porous nanocomposite microcarriers were developed for stem cell delivery and tissue engineering of bone. Incorporation of BGn significantly improved the surface bioactivity while preserving the pore structure. Apatite-mineralization, easily implemented onto the surface of BGn-added microcarriers, provided substrate conditions for MSCs to adhere, spread and actively proliferate. *In vivo* tissue compatibility and bone regeneration ability of the nanocomposite porous microcarriers were also demonstrated in a rat calvarial defect model. The mineralized surface was specifically effective in loading and releasing of biological proteins. Taken all, the porous microcarriers developed in this study are considered to have great feasibility for the cell-delivered bone tissue engineering with simultaneously delivering therapeutic proteins.

Acknowledgements: This study was supported by a grant of Priority Research Centers Program (2009-0093829), National Research Foundation, South Korea.

References

1. J.-H. Park, R. A. Pérez, G.-Z. Jin, S.-J. Choi, H.-W. Kim and I. B. Wall, *Tissue. Eng. B*., 2013, **19**, 172-179.

2. E. A. Botchwey, S. R. Pollack, E. M. Levine and C. T. Laurencin, *J. Biomed. Mater. Res*., 2001, **55**, 242-253.

3. H.-W. Kim, H.-J. Gu and H.-H. Lee, *Tissue. Eng*., 2007, **13**, 965-973.

4. S.-J. Hong, H.-S. Yu and H.-W. Kim, *Macromol, Biosci*., 2009, **9**, 639-645.

5. G.-Z. Jin, J.-H. Kim, J.-H. Park, S.-J. Choi, H.-W. Kim and I. Wall, *J. Mater. Sci. Med*., 2012, **23**, 1739-1748.

6. T. K. Kim, J. J. Yoon, D. S. Lee and T. G. Park, *Biomaterials*., 2006, **27**, 152-159.

7. X. Shi, J. Jiang, L. Sun and Z. Gan, *Colloid. Surface. B*., 2011, **85**, 73-80.

8. H.-H. Lee, S.-J. Hong, C.-H. Kim, E.-C. Kim, J.-H. Jang, H.-I. Shin and H.-W. Kim, *J. Mater. Sci. Mater. Med*., 2008, **19**, 3029-3034.

9. U. S. Shin, J.-H. Park, S.-J. Hong, J.-E. Won, H.-S. Yu and H.-W. Kim, *Mater. Lett*., 2010, **64**, 2261-2264.

10. K. W. Chun, H. S. Yoo, J. J. Yoon and T. G. Park, *Biotechnol. Prog*., 2004, **20**, 1797-1801.

11. S. J. Williams, Q. Wang, R. R. MacGregor, T. J. Siahaan, L. Stehno-Bittel and C. Berkland, *Biopolymers*., 2009, **91**, 676-685.

12. A. Liu, Z. Hong, X. Zhuang, X. Chen, Y. Cui, Y. Liu and X. Jing, *Acta. Biomater*., 2008, **4**, 1005-1015.

13. S. Labbaf, O. Tsigkou, K. H. Müller, M. M. Stevens, A. E. Porter and J. R. Jones, *Biomater*., 2011, **32**, 1010-1018.

14. A. El-Fiqi, T.-H. Kim, M. Kim, M. Eltohamy, J.-E. Won, E.-J. Lee and H.-W. Kim, *Nanoscale*, 2012, **4**, 7475-7488.

15. L. Jongpaiboonkit, T. Franklin-Ford and W. L. Murphy, *Adv. Mater*., 2009, **21**, 1960-1963.

16. J. H. Lee, J.-H. Park, Y.-R. Yun, J.-H. Jang, E.-J. Lee, W. Chrzanowski, I. B. Wall and H.-W. Kim, *J. Mater. Chem. B*., 2013, **1**, 2731-2741.

17. B. Dorj, M.-K. Kim, J.-E. Won and H.-W. Kim, *Mater. Lett*., 2011, **65**, 3559-3562.

18. J. H. Lee, J.-H. Park, A. El-Fiqi, J.-H. Kim, Y.-R. Yun, J.-H. Jang, C.-M. Han, E.-J. Lee and H.-W. Kim, *Acta Biomater.* (in press).

19. S.-A. Oh, S.-H. Kim, J.-E. Won, J.-J. Kim, U. S. Shin and H.-W. Kim, *J. Tissue. Eng*., 2010, **1**, 1-10.

20. H.-S. Yu, J.-E. Won, G.-Z. Jin and H.-W. Kim, *BioResearch. Open. Access*., 2012, **1**, 124-136.

21. R. A. Perez and H.-W. Kim, *J. Biomed. Mater. Res. A*., 2013, **101**, 1103-1112.

22. R. A. Perez, A. El-Fiqi, J.-H. Park, T.-H. Kim, J.-H. Kim and H.-W. Kim, *Acta. Biomater*., 2014, **10**, 520-530.

23. M. Sun, P. J. Kingham, A. J. Reid, S. J. Armstrong, G. Terenghi and S. Downes, *J. Biomed. Mater. Res. A*., 2009, **93**, 1470-1481.

24. M.-H. Huang, S. Li, D. W. Hutmacher, J. C. and M. Vert, *J. Appl. Polym. Sci*., 2006, **102**, 1681-1687.

25. S.-J. Hong, H.-S. Yu and H.-W. Kim, *Macromol. Biosci*., 2009, **9**, 639-645.

26. H.-S. Yu, J.-H. Jang, T.-I. Kim, H.-H. Lee and H.-W. Kim, *J. Biomed. Mater. Res. A*., 2009, **88**, 747-754.

27. H.-S. Yu, S.-J. Hong and H.-W. Kim, *Mater. Chem. Phys*., 2009, **113**, 873-877.

28. N. J. Lakhkar, I.-H. Lee, H.-W. Kim, V. Salih, I. B. Wall and J. C. Knowles, *Adv. Drug. Deliv. Rev*., 2013, **65**, 405-420.

29. S. Maeno, Y. Niki, H. Matsumoto, H. Morioka, T. Yatabe, A. Funayama, Y. Toyama, T. Taguchi and J. Tanaka, *Biomaterials*., 2005, **26**, 4847-4855.

30. J. R. Jones, O. Tsigkou, E. E. Coates, M. M. Stevens, J. M. Polak and L. L. Hench. *Biomaterials*., 2007, **28**, 1653-1663.

Figure Caption

Fig. 1. Schematic diagram showing the preparation of biofunctional nanocomposite microcarriers with porous structure as well as the utilization in bone tissue engineering after treatment of the surface: (a) Composite solution made of poly(lactic acid)/poly(caproolactone) blend with bioactive glass nanoparticle (BGn) in chloroform was mixed with camphene which was introduced as a pore generator. (b) The solution was emulsified in PVA-water bath while gentle stirring to produce spherical shaped microparticles. (c) During the emulsification, camphene was solidified with the solvent evaporation to form a bicontinuous network with the polymer phase. (d) Further stirring allowed the sublimation of camphene to leave an interconnected pore channel and the surrounding polymer networked microcarrier. The addition of BGn provides the porous microcarrier with improved bone bioactivity, such as apatite mineralization, (e) which was implemented to provide a mineralized surface on the microcarrier. (f) The mineralized surface was subsequently engineered by protein incorporation to provide a surface more mimicking the extracellular matrices of bone or therapeutic efficacy (g) to regulate stem cells for ex vivo tissue engineering or to heal/regenerate bone tissue when directly implanted.

Fig. 2. SEM image showing porous structured biopolymer microcarrier (PCL/PLDLA blended at 1/3 ratio). Spherical particles with sizes of hundreds of micrometers were produced. Highly macroporous structuring with pores approximately 50-100 □m was facilitated by using camphene which solidified to form bi-continuous network with the polymer blend and then rapidly sublimated during the spherodization process. Increasing PLDLA content was observed to reduce the possibility of spherodization and pore generation while providing better hydrophilic property, which gave a blend ratio of 1/3 optimal composition.

Fig. 3. Characteristics of the bioactive glass nanoparticle (BGn, with composition of $85SiO_2$-15CaO) which was used as the bioactive inorganic nanocomponent within the biopolymer matrix. (a) SEM and (b) TEM image showing the development of spherical nanoparticles with sizes of approximately 80-100 nm and a mesoporous structure. (c) SEM and (d) TEM image of the BGn after SBF immersion, showing the progressive mineralization of apatite nanocrystallites, which suggests high bioactivity of the nanoparticles.

Fig. 4. (a) Image showing the emulsion state of the biopolymer solutions with varying BGn

concentrations (0, 2, 5 and 10%BGn). (b,c) SEM morphologies of the nanocomposite porous microcarriers with different concentrations of BGn: 2% (b) and 10% BGn (c). (d) FT-IR spectra of the microspheres showing additional of chemical bands (Si-O-Si) related with BGn (indicated as arrows). The camphene-to-polymer ratio was set at 8. With the additions up to 10% BGnp, a spherical form of microparticles with highly porous structure was well generated, whilst a higher addition of BGn disintegrated the development of pore structure.

Fig. 5. *In vitro* apatite forming ability of the nanocomposite porous microcarriers performed within an accelerated simulated body fluid (2xSBF). SEM morphological changes of the microcarriers with varying compositions (w/o BGn and with BGn at 2, 5 and 10%) during incubation for different periods; (a) w/o BGn and (b) with 2, 5 and 10%BGn. During incubation, whilst there was little sign of the mineralization on the pure biopolymer surface, mineralized crystals were substantially developed on the outer and inner surface of the BGn-added microcarriers and the mineralization degree was increased with BGn concentration and with increasing time. The onset of mineralization detectable by SEM was approximately 7 days, 5 days and 1 day with the addition of 2%, 5% and 10%BGn, respectively. (c) FT-IR spectrum showing the development of bands related with apatite. (d) XRD pattern of 10%BGn before and after 7 days of immersion, showing development of poorly crystallized apatite phase with the immersion.

Fig. 6. *In vitro* assays of the porous microcarriers using rat MSCs to show the capacity to host and populate tissue cells for bone tissue engineering: (a) Cell proliferation rate on the microcarriers during culture for up to 7 days measured by CCK assay. (b,c) CLSM cell morphology taken on the nonmineralized (b) and mineralized (c) microcarriers at different time points (3 h, 3 days and 7 days). Stained F-actin in red and nucleus in blue. Statistical comparison between microcarrier groups showing significance difference (*$p < 0.05$, $n = 3$).

Fig. 7. *In vivo* study of the porous microcarriers performed in rat calvarium defect. Different compositions were implanted for 4 and 8 weeks and the H&E stained histological findings were compared. Experimental groups include pure blend biopolymer (biopolymer), 10%BGn-added (10%BGn), and the surface-mineralized group (mineralized). Dashed lines indicate defect margins.

Fig. 8. Micro-CT analysis, showing the volume % of neo-bone formation in the implanted groups. Results show significant improvement with 10%BGn and mineralized groups compared to biopolymer group. (*$p < 0.05$, $n = 3$). Comparison between microcarrier groups (biopolymer vs. 10%BGn vs.

mineralized at each time point).

Fig. 9. Mineralized microcarriers showing (a) effective incorporation of protein molecules (cyt C used as model protein) and (b) subsequent sustained release pattern, suggesting a potential use in delivery of proteins. (*$p < 0.05$, $n = 3$). Comparison between microcarrier groups (biopolymer vs. 10%BGn vs. mineralized at each time point). In particular, mineralized microcarrier also showed a time-dependent significance increase in cyto C release amount at all time points.

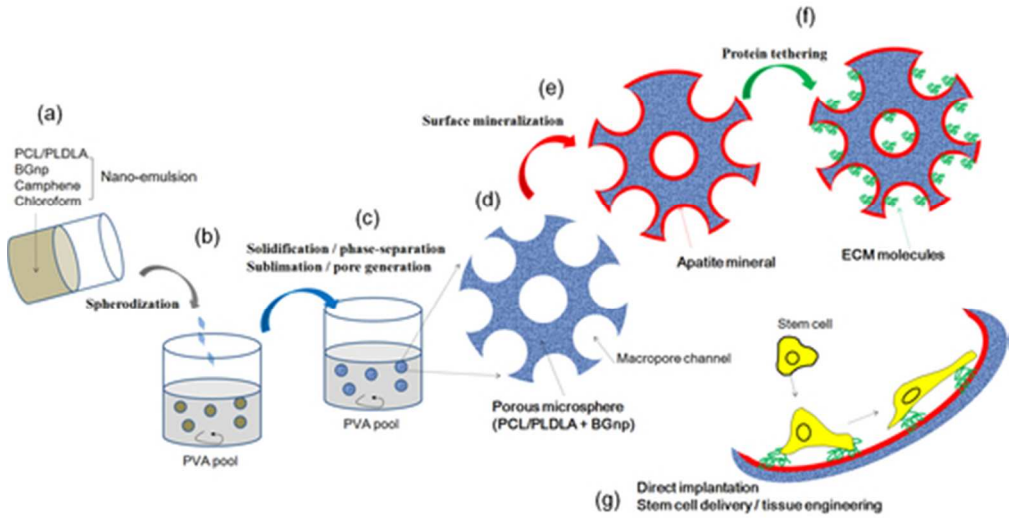

Fig. 1. Schematic diagram showing the preparation of biofunctional nanocomposite microcarriers with porous structure as well as the utilization in bone tissue engineering after treatment of the surface: (a) Composite solution made of poly(lactic acid)/poly(caproolactone) blend with bioactive glass nanoparticle (BGn) in chloroform was mixed with camphene which was introduced as a pore generator. (b) The solution was emulsified in PVA-water bath while gentle stirring to produce spherical shaped microparticles. (c) During the emulsification, camphene was solidified with the solvent evaporation to form a bicontinuous network with the polymer phase. (d) Further stirring allowed the sublimation of camphene to leave an interconnected pore channel and the surrounding polymer networked microcarrier. The addition of BGn provides the porous microcarrier with improved bone bioactivity, such as apatite mineralization, (e) which was implemented to provide a mineralized surface on the microcarrier. (f) The mineralized surface was subsequently engineered by protein incorporation to provide a surface more mimicking the extracellular matrices of bone or therapeutic efficacy (g) to regulate stem cells for ex vivo tissue engineering or to heal/regenerate bone tissue when directly implanted.
44x23mm (300 x 300 DPI)

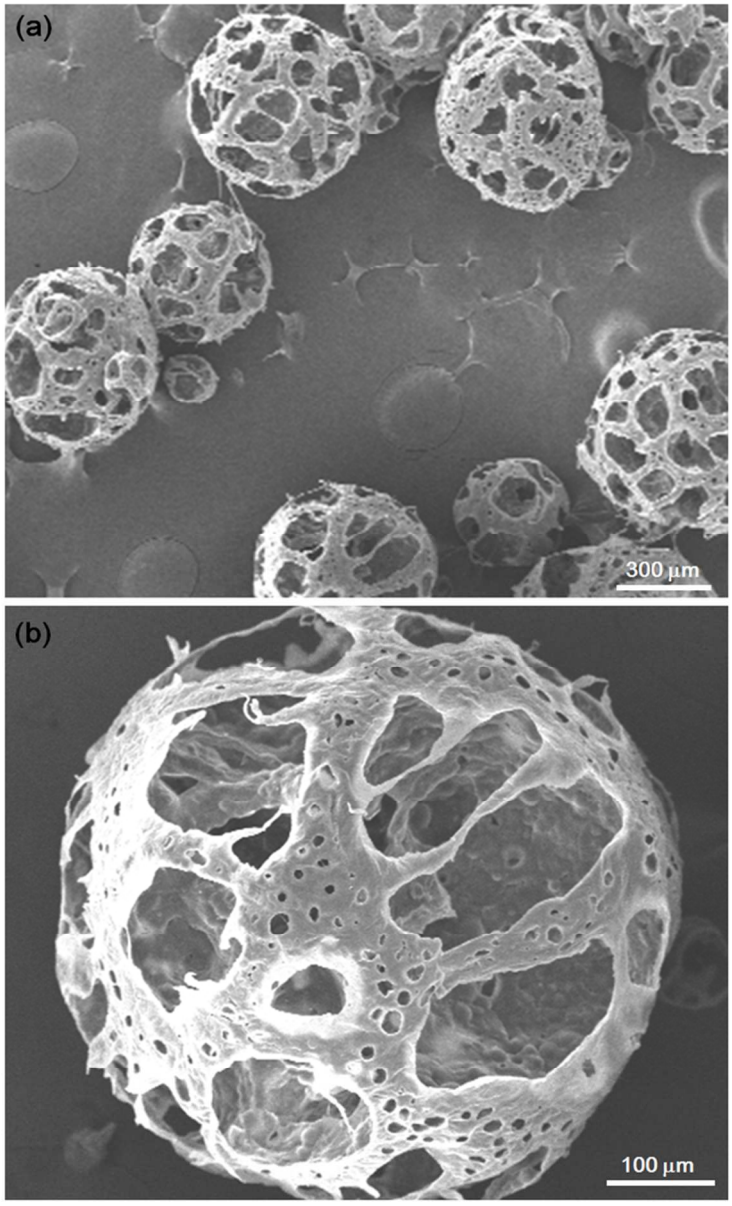

Fig. 2. SEM image showing porous structured biopolymer microcarrier (PCL/PLDLA blended at 1/3 ratio). Spherical particles with sizes of hundreds of micrometers were produced. Highly macroporous structuring with pores approximately 50-100 μm was facilitated by using camphene which solidified to form bi-continuous network with the polymer blend and then rapidly sublimated during the spherodization process. Increasing PLDLA content was observed to reduce the possibility of spherodization and pore generation while providing better hydrophilic property, which gave a blend ratio of 1/3 optimal composition.
56x92mm (300 x 300 DPI)

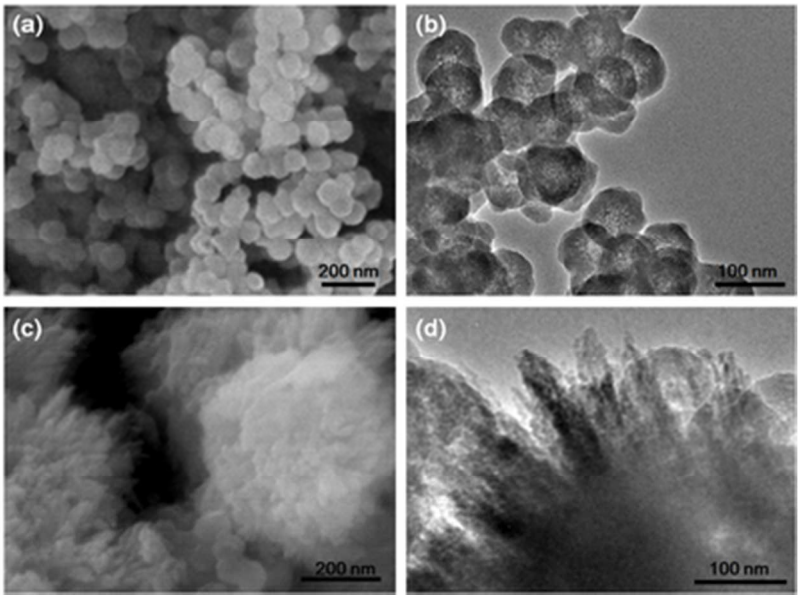

Fig. 3. Characteristics of the bioactive glass nanoparticle (BGn, with composition of 85SiO2-15CaO) which was used as the bioactive inorganic nanocomponent within the biopolymer matrix. (a) SEM and (b) TEM image showing the development of spherical nanoparticles with sizes of approximately 80-100 nm and a mesoporous structure. (c) SEM and (d) TEM image of the BGn after SBF immersion for 7 days, showing the progressive mineralization of apatite nanocrystallites, which suggests high bioactivity of the nanoparticles.
33x24mm (300 x 300 DPI)

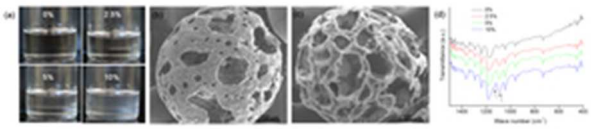

Fig. 4. (a) Image showing the emulsion state of the biopolymer solutions with varying BGn concentrations (0, 2, 5 and 10%BGn). (b,c) SEM morphologies of the nanocomposite porous microcarriers with different concentrations of BGn: 2% (b) and 10% BGn (c). (d) FT-IR spectra of the microspheres showing additional of chemical bands (Si-O-Si) related with BGn (indicated as arrows). The camphene-to-polymer ratio was set at 8. With the additions up to 10% BGnp, a spherical form of microparticles with highly porous structure was well generated, whilst a higher addition of BGn disintegrated the development of pore structure.
25x5mm (300 x 300 DPI)

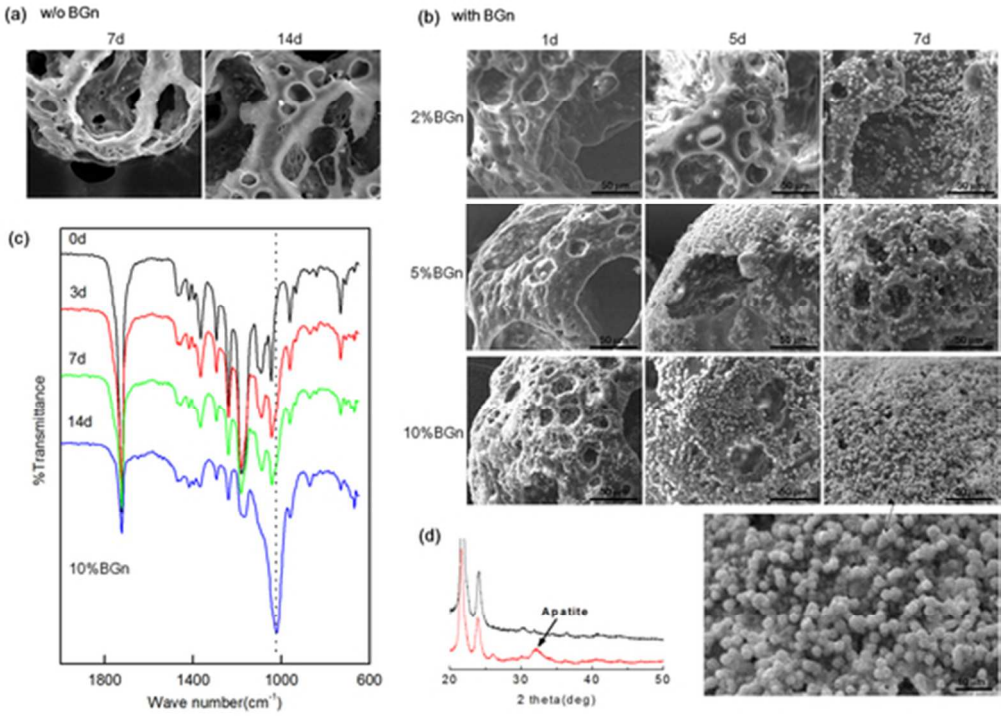

Fig. 5. In vitro apatite forming ability of the nanocomposite porous microcarriers performed within an accelerated simulated body fluid (2xSBF). SEM morphological changes of the microcarriers with varying compositions (w/o BGn and with BGn at 2, 5 and 10%) during incubation for different periods; (a) w/o BGn and (b) with 2, 5 and 10%BGn. During incubation, whilst there was little sign of the mineralization on the pure biopolymer surface, mineralized crystals were substantially developed on the outer and inner surface of the BGn-added microcarriers and the mineralization degree was increased with BGn concentration and with increasing time. The onset of mineralization detectable by SEM was approximately 7 days, 5 days and 1 day with the addition of 2%, 5% and 10%BGn, respectively. (c) FT-IR spectrum showing the development of bands related with apatite. (d) XRD pattern of 10%BGn before and after 7 days of immersion, showing development of poorly crystallized apatite phase with the immersion.
45x32mm (300 x 300 DPI)

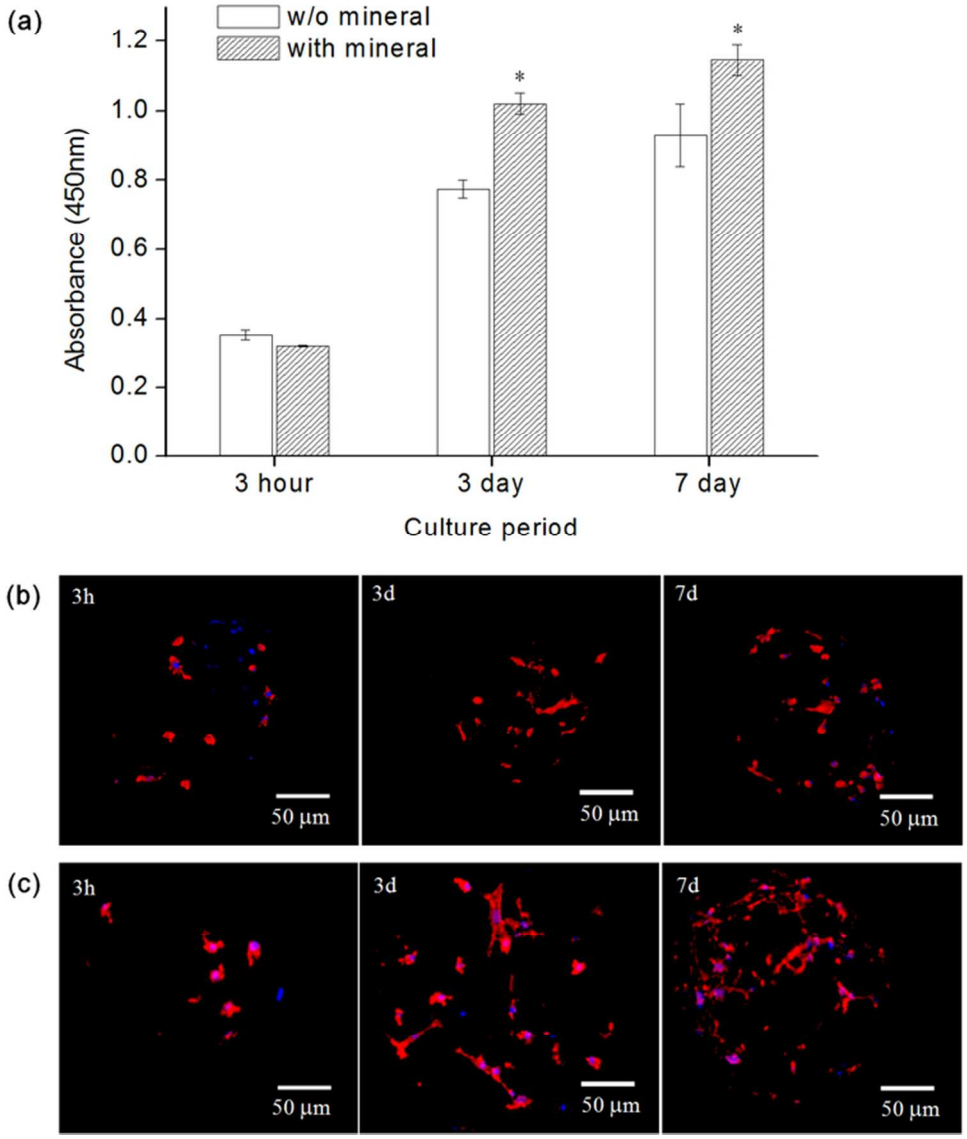

Fig. 6. In vitro assays of the porous microcarriers using rat MSCs to show the capacity to host and populate tissue cells for bone tissue engineering: (a) Cell proliferation rate on the microcarriers during culture for up to 7 days measured by CCK assay. (b,c) CLSM cell morphology taken on the nonmineralized (b) and mineralized (c) microcarriers at different time points (3 h, 3 days and 7 days). Stained F-actin in red and nucleus in blue. Statistical comparison between microcarrier groups showing significance difference (*$p < 0.05$, $n = 3$).
65x79mm (300 x 300 DPI)

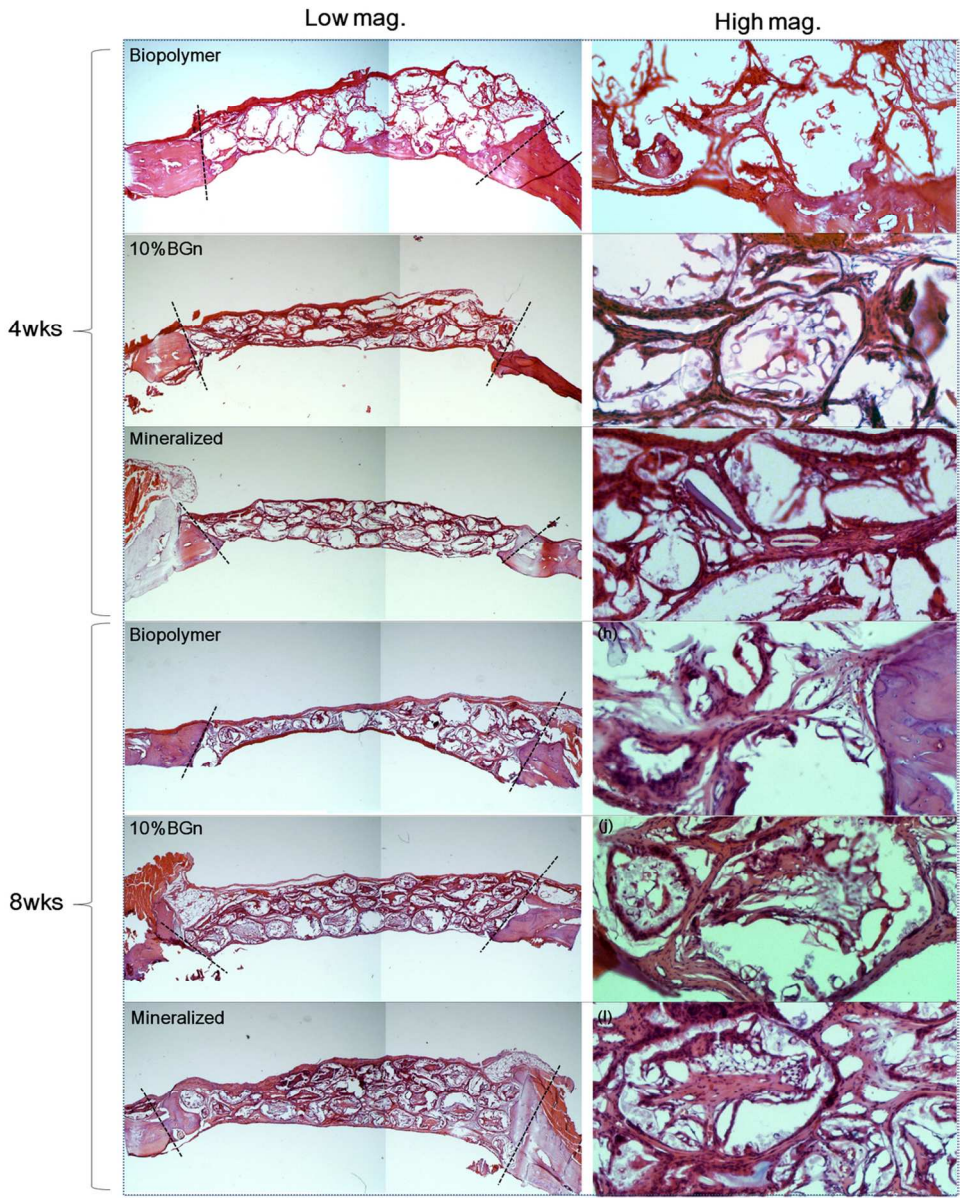

Fig. 7. In vivo study of the porous microcarriers performed in rat calvarium defect. Different compositions were implanted for 4 and 8 weeks and the H&E stained histological findings were compared. Experimental groups include pure blend biopolymer (biopolymer), 10%BGn-added (10%BGn), and the surface-mineralized group (mineralized). Dashed lines indicate defect margins.
105x130mm (300 x 300 DPI)

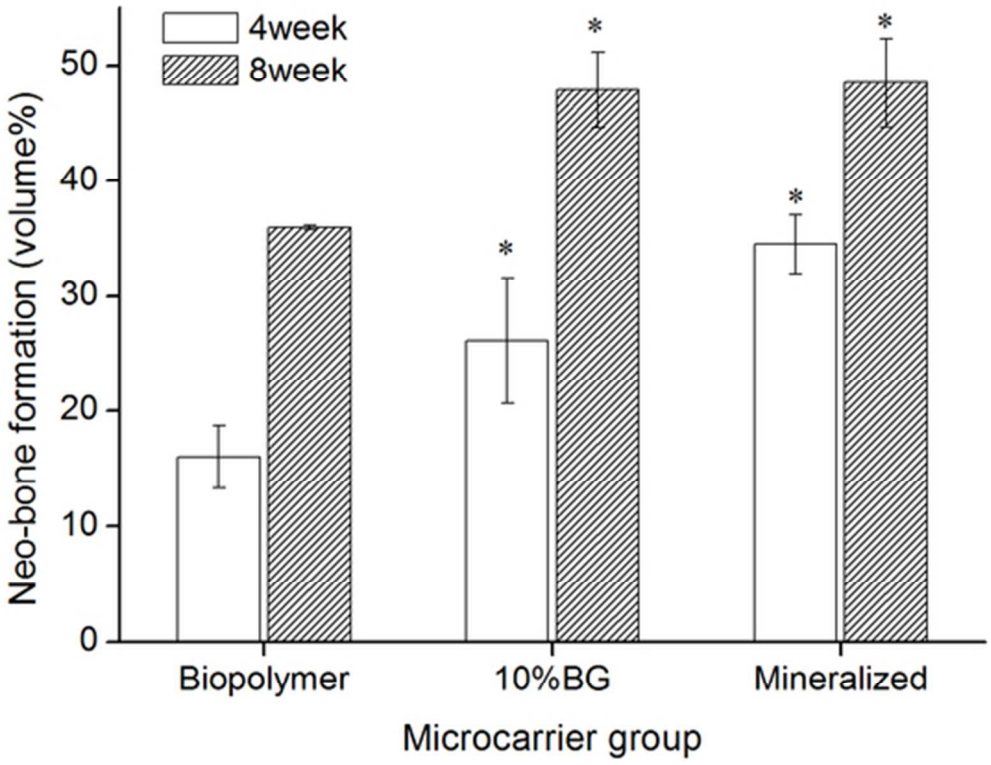

Fig. 8. Micro-CT analysis, showing the volume % of neo-bone formation in the implanted groups. Results show significant improvement with 10%BGn and mineralized groups compared to biopolymer group. (*p < 0.05, n = 3). Comparison between microcarrier groups (biopolymer vs. 10%BGn vs. mineralized at each time point).
45x36mm (300 x 300 DPI)

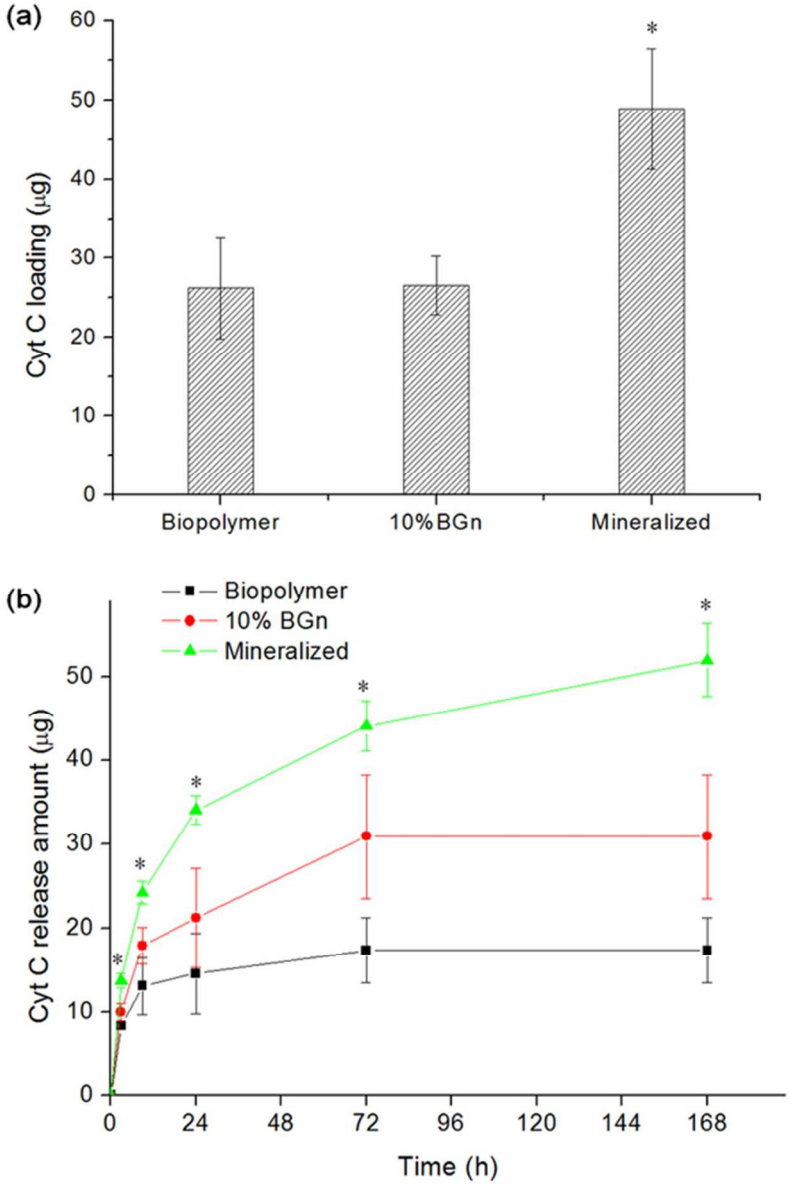

Fig. 9. Mineralized microcarriers showing (a) effective incorporation of protein molecules (cyt C used as model protein) and (b) subsequent sustained release pattern, suggesting a potential use in delivery of proteins. (*$p < 0.05$, $n = 3$). Comparison between microcarrier groups (biopolymer vs. 10%BGn vs. mineralized at each time point). In particular, mineralized microcarrier also showed a time-dependent significance increase in cyto C release amount at all time points.
50x74mm (300 x 300 DPI)